https://doi.org/10.5194/egusphere-2025-5846
Preprint. Discussion started: 5 December 2025

Turbulent Mixing in Patagonian Fjords and Channels

Marcela Rojas-Celis [1,9], Manuel I. Castillo [2,9], Iván Pérez-Santos [3,4], Carmen Barrios-Guzmán[5,7], José Garcés-Vargas [6,10], Alicia Guerrero[7], Mauricio F. Landaeta [2,8,11], Andrea Piñones[4,6,10,11], Maritza Sepúlveda [5,7]

[1]Programa de Magister en Oceanografía, Universidad de Valparaíso y Pontificia Universidad Católica de Valparaíso, Chile.
[2]Centro de Observación y Análisis del Océano Costero (COSTA-R), Universidad de Valparaíso, Valparaíso, Chile.
[3]Centro i~mar, Universidad de Los Lagos, Puerto Montt, Chile.
[4]COPAS COASTAL Oceanographic Research Center, Universidad de Concepción, Concepción, Chile.
[5]Centro de Investigación y Gestión de Recursos Naturales (CIGREN), Universidad de Valparaíso, Valparaíso, Chile
[6]Instituto de Ciencias Marinas y Limnológicas, Facultad de Ciencias, Universidad Austral de Chile.
[7]Laboratorio de Ecología y Conservación de Mamíferos Marinos (LECMMAR), Universidad de Valparaíso, Chile.
[8]Laboratorio de Ictiología e Interacciones Biofísicas (LABITI), Instituto de Biología, Facultad de Ciencias, Universidad de Valparaíso, Valparaíso, Chile.
[9]Laboratorio de Oceanografía Física y Satelital (LOFISAT) , Universidad de Valparaíso, Chile.
[10]Centro FONDAP de Investigación en Dinámica de Ecosistemas Marinos de Altas Latitudes (IDEAL), Universidad Austral de Chile, Chile.
[11]Millennium Institute Biodiversity of Antarctic and Sub-Antarctic Ecosystems (BASE), Santiago, Chile.

Correspondence to: manuel.castillo@uv.cl

Abstract. The fjords and channels of Chilean Patagonia form a complex estuarine system where freshwater input, tidal currents, and stratification interact to modulate vertical mixing. We combined velocity microstructure profiles (VMP-250) and CTD-SRDL observations collected between 2023 and 2025 to quantify turbulent kinetic energy dissipation (ε) and vertical diffusivity (K_{shear}) across northern (42–46°S) and southern (52–55°S) Chilean Patagonia. Dissipation rates spanned 10^{-9}–10^{-5} W kg^{-2} with maxima near sills and narrow passages such as Paso Desertores, where semidiurnal tides dominate energy input. Northern Patagonia exhibited seasonal stratification driven by freshwater inputs, while southern Patagonia remained weakly stratified and vertically well mixed throughout the year, aided by strong tidal currents and westerly winds. The tidal mixing parameter h/U^3 indicated that semidiurnal tides account for ~97% of energy dissipation in the north and ~77% in the south. These findings highlight the strong spatial heterogeneity of turbulent mixing in Patagonian fjords and the key role of the interaction between tidal forcing and stratification in controlling vertical exchange. The results provide a framework for understanding how fjord systems may respond to changing freshwater inputs and atmospheric forcing under a warming climate.

https://doi.org/10.5194/egusphere-2025-5846
Preprint. Discussion started: 5 December 2025

1 Introduction

Turbulent mixing is a fundamental process in the ocean that regulates the vertical exchange of heat, salt, momentum, and biogeochemical tracers across density gradients. It arises from the chaotic and nonlinear nature of fluid motion, a hallmark of geophysical flows such as the atmosphere and the ocean (Tennekes & Lumley, 1972; Pope, 2000). Turbulence enhances diffusivity and accelerates energy and matter transfer across scales, making it an efficient mixing mechanism (Gregg, 1987; Thorpe, 2005). Although turbulent motion is intermittent and localized, its cumulative effect shapes the large-scale structure and energetics of the ocean, influencing global circulation, heat redistribution, and climate regulation (Munk & Wunsch, 1998; MacKinnon et al., 2017). Understanding the mechanisms and variability of turbulent mixing is therefore essential for constraining energy budgets and vertical transport in the ocean, particularly in stratified and semi-enclosed systems, like estuaries or fjords, where turbulent energy dissipation can increase by up to three orders of magnitude relative to the open ocean (Gregg, 1987). In such environments, small-scale processes exert a disproportionate influence on water mass transformation and ecosystem dynamics (Ferron et al., 2014; Waterhouse et al., 2014).

The Chilean Patagonia, contain one of the largest fjord networks in the world, from Reloncaví Fjord (41.5°S) to Cape Horn (55.9°S) (Fig. 1), covering approximately 240,000 km² (Pantoja et al., 2011; Silva & Palma, 2008). Patagonian fjords are characterized by a markedly irregular coastal morphology and bathymetry which includes islands, peninsulas, seamounts, and sills, which influence connectivity between basins and sub-basins and affect biogeochemical and biological processes (Schneider et al., 2014; Devine, 1983; Landaeta et al., 2011). Considering these complex differences in bathymetry, hydrography, and circulation patterns among basins, based on geographical features a subdivision in zones was first proposed by Pickard (1971): the Northern, Central, and Southern Patagonia. Then a most complex classification of the region was based on the vertical and horizontal circulation schemes derived from observed water properties which describe a highly stratified system where estuarine and subantarctic waters interact across multiple layers (surface, intermediate, and bottom) constrained by topographic sills and constrictions. Such features act as partial barriers that modulate and limits water exchange and oxygen renewal between fjord basins, creating distinct hydrographic regimes along the Patagonian coast (Sievers et al., 2002; Valdenegro & Silva, 2003; Sievers and Silva, 2008).

Northern Patagonia extends from the Reloncaví Fjord (41°5'S, 72°23'W) to Laguna San Rafael (46°67'S, 73°53'W). This area is characterized by a dense network of interconnected fjords and channels separated by shallow sills and narrow passages. Communication with the Pacific Ocean occurs mainly through Guafo Mouth (~50 km wide, between Chiloé Island and the Chonos Archipelago), while more restricted exchanges take place through the Chacao Channel and inner archipelago passages (Cáceres et al., 2003). The hydrography of this region is dominated by a strong estuarine circulation, driven by intense freshwater from precipitation and rivers discharge due to seasonal snow melting from the Andes Cordillera, combined with limited oceanic intrusion. As a result, surface waters are typically cold and low in salinity ($S \approx 0 - 31$ g kg^{-1}), forming a buoyant

https://doi.org/10.5194/egusphere-2025-5846
Preprint. Discussion started: 5 December 2025

estuarine water (EW) layer that flows seaward above a more saline Subantarctic Water (SAAW) which ranged between 31–33 g kg^{-1}, entering at intermediate depths through Boca del Guafo (Sievers & Silva, 2008). This salinities differences promotes strong vertical stratification and constrains the vertical mixing mostly in the inner-sea of Chiloé where steep bathymetry, shallow sills and constrictions (e.g., Paso Desertores-Apiao) could excite internal waves, enhancing turbulent mixing (Silva & Palma, 2008; Cáceres et al., 2003).

The region experiences large tidal amplitudes and energetic tidal currents. In Puerto Montt, the tidal amplitude exceeds 7 m due to barotropic resonance of M_2 within the inner sea of Chiloé (Aiken, 2008), whereas at Boca del Guafo and along most of the open coast, the tidal amplitude is around 2 m. The combination of high freshwater input, restricted oceanic exchange, and strong tidal forcing makes Northern Patagonia a highly dynamic transition zone where physical processes strongly modulate biogeochemical gradients.

Southern Patagonia, by contrast, extends across fjords, channels, and straits from the Strait of Magellan (52°31'S) to Cape Horn (55°9'S). The morphology of this region presented a connection between both Pacific and Atlantic Oceans, which resulted in a dynamic exchange of water masses. The Magellan Strait is the most prominent feature in the region with an interoceanic passage subdivided into micro-basins by narrow constrictions known as the First and the Second Narrows, each with distinct morpho-bathymetric and hydrographic characteristics (Brun et al., 2020; Valdenegro & Silva, 2003). The hydrographic structure here reflects the interplay between Pacific Subantarctic Water (PSW) and Atlantic Subantarctic Water (SAAW), which interact beneath a relatively thin surface layer of freshwater (FW) derived from glacial melt and riverine input, particularly from the Darwin Range. This stratification produces a two-layer circulation pattern: a seaward flow of diluted surface waters and a compensating inflow of subantarctic waters at intermediate and deep levels (Sievers et al., 2002; Palma & Silva, 2004). Unlike the northern region, Southern Patagonia experiences weaker tidal amplitudes (typically <2 m) and lower freshwater discharge, but larger-scale oceanic and atmospheric forcings play a more prominent role. The inflow of subantarctic and occasionally Antarctic waters contributes to higher nutrient availability and more efficient ventilation of deep basins (Valdenegro & Silva, 2003). Consequently, while the northern fjords exhibit strong stratification and localized mixing "hotspots," the southern channels and straits tend to be better ventilated and more directly influenced by open-ocean conditions (Carranza et al., 2017; Sassi and Palma, 2017).

This study compares the fjord systems of northern and southern Patagonia to investigate how regional differences in bathymetry, tide, wind, and freshwater inputs modulate turbulent mixing. Using velocity microstructure and hydrographic data, we evaluate the role of shallow sills as local mixing hotspots, their capacity for deep water ventilation, and their broader implications for fjord dynamics in each region.

https://doi.org/10.5194/egusphere-2025-5846
Preprint. Discussion started: 5 December 2025

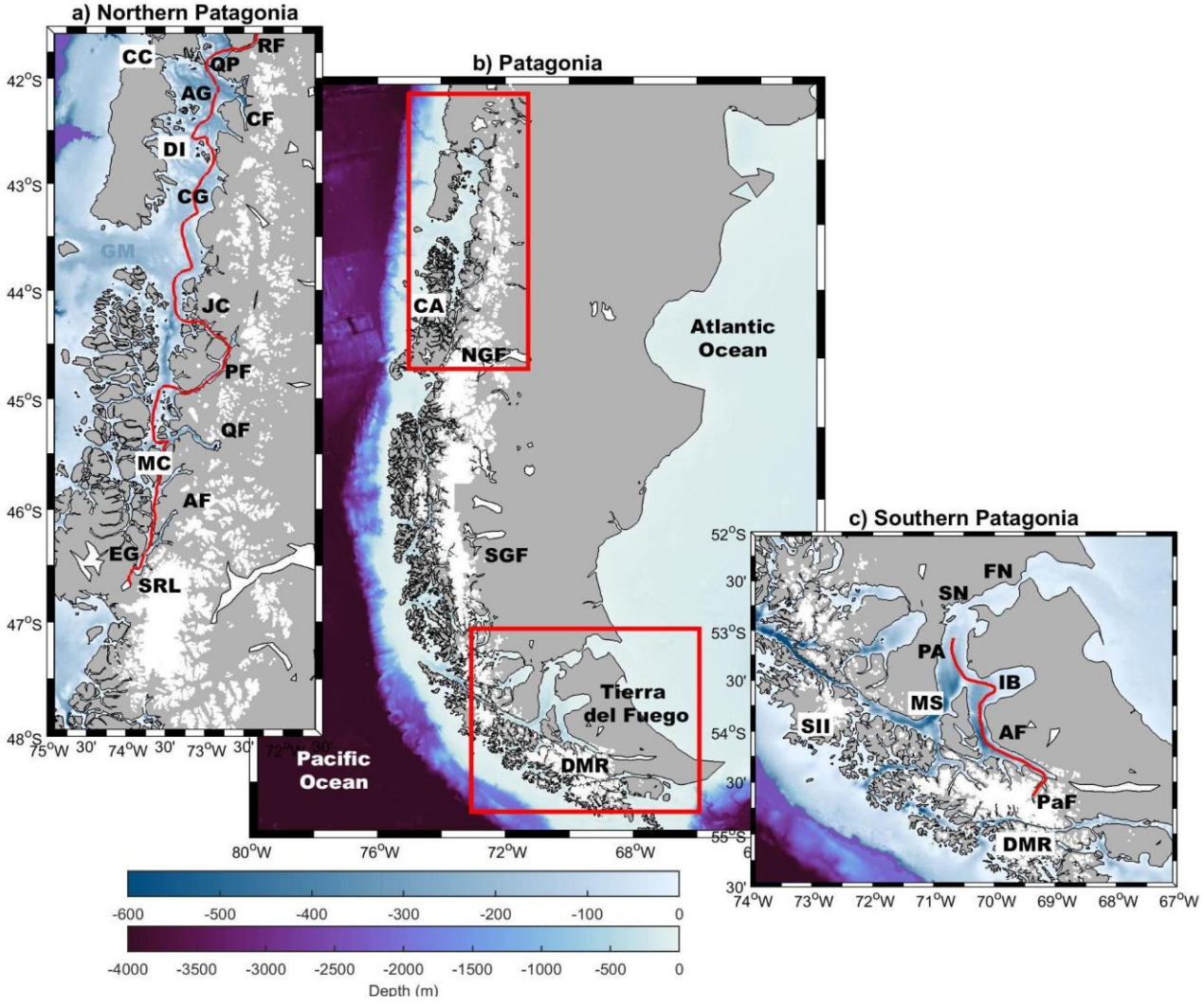

Figure 1. Map of Chilean Patagonia. The color scale indicates bathymetry (in meters). The red lines represent the oceanographic tracks sampled during the studies. (a) Northern Patagonia, extending from Reloncaví Fjord to San Rafael Lagoon. (b) Patagonia region, highlighting the transition between the Pacific and Atlantic oceans and the location of the Northern and Southern red boxes corresponding to panels (a) and (c). (c) Southern Patagonia, including the Strait of Magellan and adjacent channels. Geographic names are indicated with black labels. Acronyms in the map correspond to the following locations: RF – Reloncaví Fjord; CC – Chacao Channel; QP – Queullín Passage; AG – Ancud Gulf; CF – Comau Fjord; DI – Desertores Islands; GM – Guafo Mouth; JC – Jacaf Channel; PF – Puyuhuapi Fjord; MC – Moraleda Channel; CA – Chonos Archipielago; QF – Quitralco Fjord; AF – Aysén Fjord; SRL – San Rafael Lagoon; NGF – Northern Glacial Field; SGF – Southern Glacial Field; FN – First Narrow; SN – Second Narrow; IB – Inútil Bay; AF – Almirantazgo Fjord; MS – Magellan Strait; SII – Santa Ines Icefield; DMR – Darwin Mountain Range; PaF – Parry Fjord.

https://doi.org/10.5194/egusphere-2025-5846
Preprint. Discussion started: 5 December 2025

2 Material and Methods

2.1 Hydrography data: CTD-SRDL Measurements

To extend spatial coverage to remote areas of southern Magallanes, autonomous Conductivity–Temperature–Depth Satellite Relay Data Loggers (CTD-SRDLs, https://www.smru.st-andrews.ac.uk/Instrumentation/, Fig. 2a) were deployed on southern elephant seals (*Mirounga leonina*) (six individuals in 2024 and thirteen in 2025) (Table 1, Fig. 1). These large, deep-diving pinnipeds served as natural oceanographic samplers, collecting high-resolution hydrographic profiles across extensive and otherwise inaccessible regions. Adult females, subadult males and juveniles were captured and instrumented at Bahía Jackson (Tierra del Fuego, Chile) following established animal-handling and ethical protocols (Field et al., 2012).

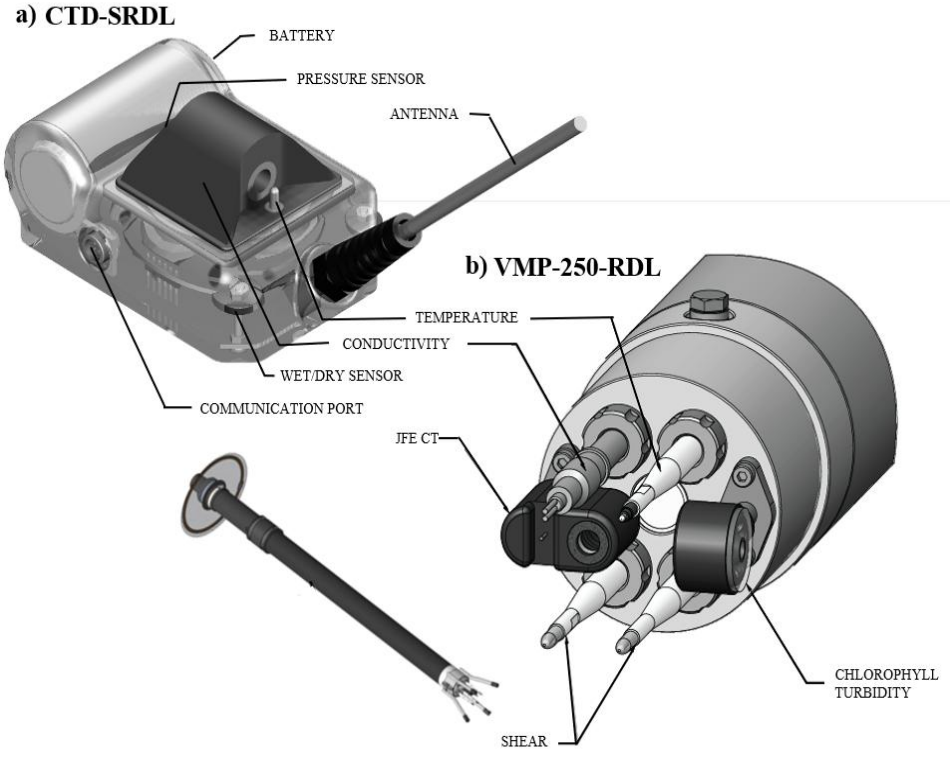

Figure 2. Schematic diagram of the oceanographic instrumentation used in this study. a) CTD-SRDL system equipped with conductivity, temperature, and depth sensors. b) Microstructure profiler used to obtain high-resolution vertical profiles of turbulence and stratification parameters. Key sensor components are labeled in both instruments.

https://doi.org/10.5194/egusphere-2025-5846
Preprint. Discussion started: 5 December 2025

After release, the seals undertook foraging trips during which the CTD-SRDLs recorded vertical profiles of temperature, conductivity, and pressure down to approximately 2000 m. Onboard algorithms detected the deepest point of each dive, initiating high-frequency sampling during ascent until surfacing (Boehme et al., 2009). Pressure sensors and wet–dry switches allowed reconstruction of dive behavior and identification of individual records (Fedak et al., 2002). Data was stored internally and transmitted via the ARGOS satellite system, providing near real-time observations of both oceanographic conditions and diving activity.

2.2 Hydrography data: CTD and Microturbulence Measurements

High-resolution vertical profiles of temperature, salinity, dissolved oxygen, and turbulent shear were obtained using a microstructure profiler (VMP-250-RDL, Rockland Scientific) (Table 1, Fig. 1) and complementary sensors (Fig. 2b). Turbulent kinetic energy dissipation (ε) was calculated from vertical shear measurements according to:

$$\varepsilon = 7.5\upsilon\left(\frac{\partial u}{\partial z}\right)^2 \quad (1)$$

where ε is the turbulent kinetic energy dissipation rate ($m^2\ s^{-3}$), ν is the molecular viscosity of seawater ($m^2\ s^{-1}$), and $\left(\frac{\partial u}{\partial z}\right)^2$ is the variance of the vertical shear. Dissipation rates were estimated below 5 m depth to minimize vessel effects. Vertical diffusivity (K_{shear}) was calculated following Osborn (1980):

$$K_{shear} = \Gamma\frac{\varepsilon}{N^2} \quad (2)$$

where N^2 is the Brunt–Väisälä (buoyant) frequency, and Γ is the mixing efficiency. For cases where ε/N^2 exceeds 100, the formulation by Shih et al. (2005) was applied. All profiles were first checked by visual inspection to ensure consistency across sensors. Hydrographic data was quality-controlled, averaged over 1 m depth intervals, and interpolated to uniform depth grids to construct vertical transects of all measured variables.

https://doi.org/10.5194/egusphere-2025-5846
Preprint. Discussion started: 5 December 2025

Table 1. Oceanographic campaigns carried out in Patagonian fjords and channels between 2023 and 2025. In northern Patagonia (PN) and southern Patagonia (PS). Each cruise season indicates the number of stations with turbulence profiles and hydrographic measurements (temperature, salinity, and dissolved oxygen) including the CTD–SRDL data collected by seal-borne instruments.

Cruise Season	Date (dd-mm)	Stations	Measurements
PN-Summer-2023	March 04-19	52	Temperature, Salinity, and DO2
		47	Turbulence
PN-Fall-2023	May 30-June 14	56	Temperature, Salinity, and DO2
		54	Turbulence
PN-Winter-2023	August 06-20	58	Temperature, Salinity, and DO2
		57	Turbulence
PN-Fall/Winter-2024	June 23-July 07	46	Temperature, Salinity, and DO2
		44	Turbulence
PN-Winter-2024	July 31-August 21	42	Temperature, Salinity, and DO2
		42	Turbulence
PN-Spring-2024	December 06-19	50	Temperature, Salinity, and DO2
		43	Turbulence
PS-Summer-2024	January 26-March 19	747	Temperature and Salinity
PS-Fall-2024	March 21-May 31	2672	Temperature and Salinity
PS-Winter-2024	July 31-August 21	380	Temperature and Salinity
CIMAR Fiordos 27 Winter-2024	August 24-September 10	26	Temperature, Salinity, and DO2
		26	Turbulence
PS-Summer-2025	January 23-March 19	1958	Temperature and Salinity
PS-Fall-2025	March 20-June 20	2345	Temperature and Salinity
PS-Winter-2025	June 21-July 18	487	Temperature and Salinity

https://doi.org/10.5194/egusphere-2025-5846
Preprint. Discussion started: 5 December 2025

2.3 Quantification of stratification, mixing and tidal dissipation

Water column stratification was assessed through the Brunt–Väisälä frequency:

$$N^2 = -\frac{g}{\rho}\frac{\partial \rho}{\partial z} \quad (4)$$

where g is the gravitational acceleration ($m\ s^{-2}$), ρ is the potential density (kg m^{-3}), and $\partial\rho/\partial z$ is the vertical density gradient. N^2 was expressed in cycles per hour (cph), with values near 0 indicating a well-mixed column. The degree of stratification of the water column was evaluated using the integrated stratification parameter (n_s), defined by Haralambidou et al. (2010) as:

$$n_s = \frac{S_{50m} - S_{sirface}}{1/2(S_{50m} + S_{surface})} \quad (5)$$

where $S_{surface}$ and S_{50m} are the salinity values at the surface and at 50 m depth, respectively. According to Haralambidou et al. (2010), values of $n_s < 0.2$ indicate well-mixed conditions, $0.2 < n_s < 1$ corresponds to partially mixed conditions, and $n_s > 1$ denote a stratified water column.

Tidal forcing was estimated from the TPXO9-atlas-v5 (Egbert and Erofeeva, 2002) model and validated with IOC sea-level records. The Simpson & Hunter (1974) tidal mixing parameter (S) was computed as:

$$S = \frac{H}{U^3} \quad (6)$$

where U is the barotropic tidal current. Tidal energy dissipation at the seabed was estimated using:

$$\beta_{tidal} = \rho C_d U^3/h \quad (7)$$

with ρ seawater density and C_d (0.0025) the bottom drag coefficient. This approach identifies regions of strong tidally driven mixing, such as sills and constrictions, providing a proxy for dissipation where detailed stress measurements are unavailable.

https://doi.org/10.5194/egusphere-2025-5846
Preprint. Discussion started: 5 December 2025

3 Results

3.1 Seasonal patterns of hydrography in northern and southern Patagonia

In northern Patagonia, the density distribution along the transect from San Rafael Lagoon to Reloncaví Fjord exhibited a marked seasonal variability in both vertical structure and spatial patterns. During summer 2023, an upper low-density surface estuarine layer (~21–23 kg m^{-3}) was observed at San Rafael Lagoon (1 km) and Quitralco Fjord (140 km), gradually increasing northward and reaching values >26 kg m^{-3} in the Chiloé Island Sea as well as in the Comau and Reloncaví fjords. In winter 2023 and 2024, denser waters (>26 kg m^{-3}) extended deeper into Puyuhuapi Fjord. In spring 2024, the decrease in surface density (~23–24 kg m^{-3}) suggests a renewed freshwater influence extending from San Rafael Lagoon to Jacaf Channel and into the Reloncaví and Comau fjords, likely associated with snowmelt or increased precipitation (Fig. 3).

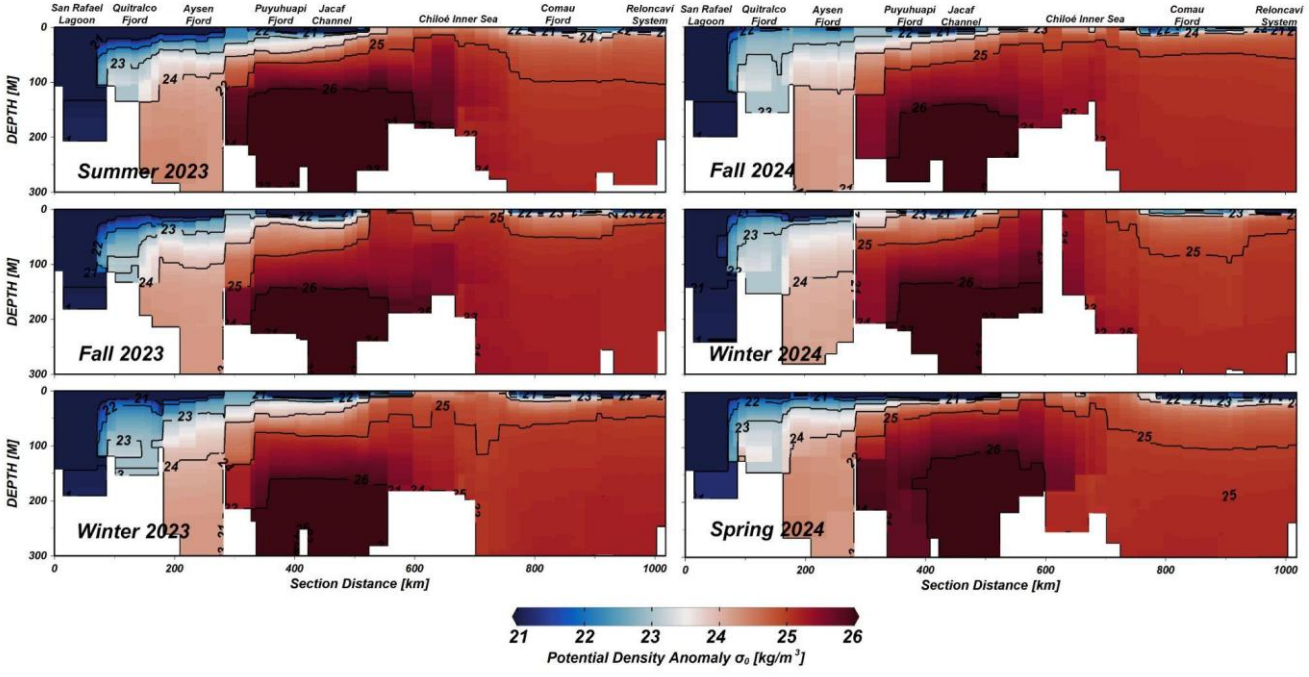

Figure 3. Potential density anomaly along the northern Patagonia region for summer, fall, winter and spring 2024/25. The along-fjord distance is referenced to San Rafael lagoon (Fig. 1).

The vertical structure displayed a well-mixed deep layer separated from the surface by a pronounced gradient, particularly during spring and summer. In the western sector (San Rafael to Puyuhuapi), density values were lower and exhibited greater seasonal variability. In contrast, the eastern sector (Jacaf Channel to Reloncaví Fjord) was dominated by denser waters influenced by oceanic intrusions (Fig. 3).

https://doi.org/10.5194/egusphere-2025-5846
Preprint. Discussion started: 5 December 2025

Seasonal variability was also evident in the Brunt–Väisälä frequency (N^2). In spring 2024 and summer 2023, maximum values > 60 cycles h^{-1} were observed in the upper 15 m, indicating strong surface stratification. Conversely, during fall and winter, N^2 decreased to < 20 cycles h^{-1} across most of the transect, reflecting reduced vertical stability and enhanced turbulent mixing potential. The region between Aysén Fjord and Jacaf Channel was particularly stratified in summer, whereas winter and fall were characterized by deep mixing throughout the system (Fig. 4).

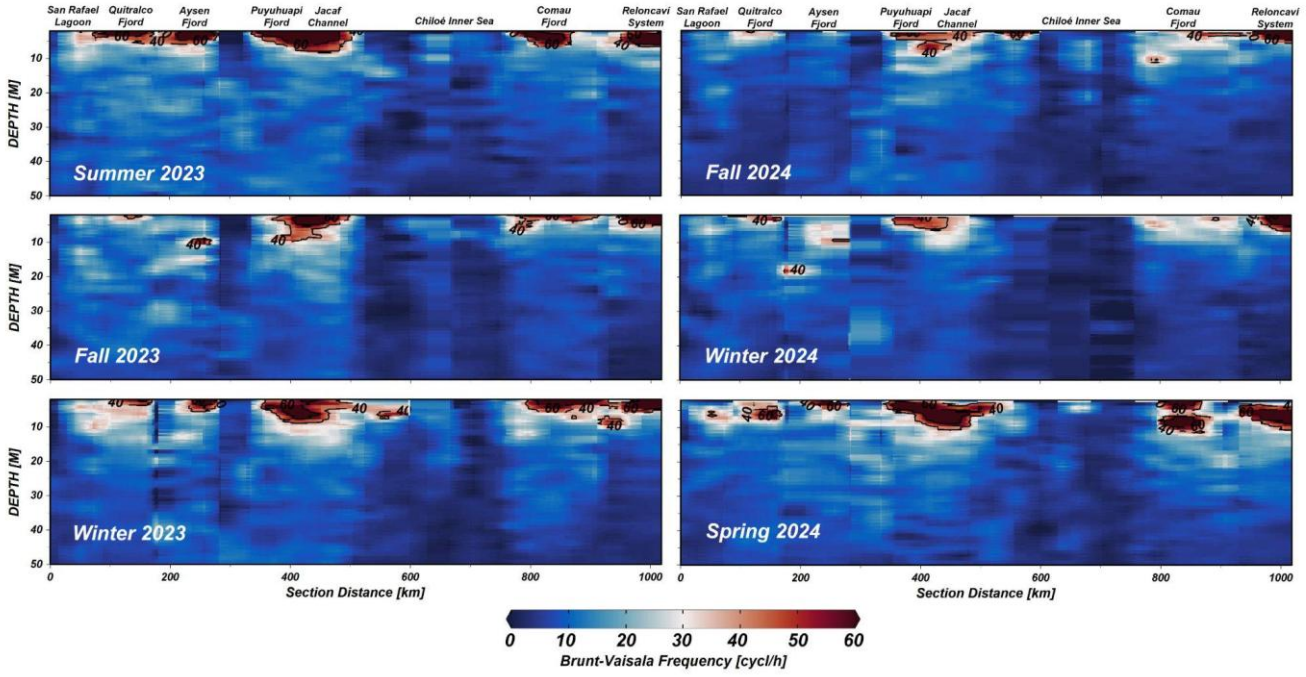

Figure 4. Brunt-Väisälä frequency (first 50 m) along the northern Patagonia region for summer, fall, winter and spring of 2024/25. The along-fjord distance is referenced to San Rafael lagoon (Fig. 1).

In southern Patagonia (Fig. 5), the density distribution along the transect from Parry Fjord to Punta Arenas exhibited a relatively homogeneous vertical structure throughout the study period, dominated by dense waters (>23 kg m^{-3}), particularly in the northern portion of the transect. During summer 2024, the water column showed densities ranging from 21 to 24 kg m^{-3} from the surface to 200 m, with a vertical gradient. In fall 2024, the 24 kg m^{-3} isopycnal deepened, reaching up to 110 m in the southern areas (Inútil Bay and Parry Fjord). In winter 2024, surface density slightly decreased (~22–23 kg m^{-3}) in the southern section (Parry Fjord), while the northern section remained more stable. For summer 2025, a more pronounced pattern emerged: lower surface densities (~22–23 kg m^{-3}) were found from Parry Fjord to Almirantazgo Fjord, followed by an increase towards the north, reaching >24 kg m^{-3} near Punta Arenas. This pattern continued into fall 2025, where the density structure was

https://doi.org/10.5194/egusphere-2025-5846
Preprint. Discussion started: 5 December 2025

characterized by a denser subsurface intrusion (~24 kg m^{-3}) between 50 and 150 m in the central transect. In winter 2025, the density structure appeared less defined but remained homogeneously dense (~23–24 kg m^{-3}) throughout the water column. N^2 ranged from 0 to 30 cycles h^{-1}, showing less marked seasonal variability. In summer 2024, moderate N^2 values (~12 cycles h^{-1}) were observed in the upper 50 m, especially between Almirantazgo Fjord and Parry Fjord. Stratification progressively weakened during fall and winter 2024, with values <6 cycles h^{-1} across most of the transect. In summer 2025, higher N^2 values (>15 cycles h^{-1}) reappeared in the southern surface layer. Fall 2025 exhibited a persistent intermediate stratified layer (6–9 cycles h^{-1}) in the first 50 m in the southern surface layer until Inútil Bay. Overall, Southern Patagonia displayed less vertical and seasonal variability than Northern Patagonia, resulting in a more homogeneous and weakly stratified water column.

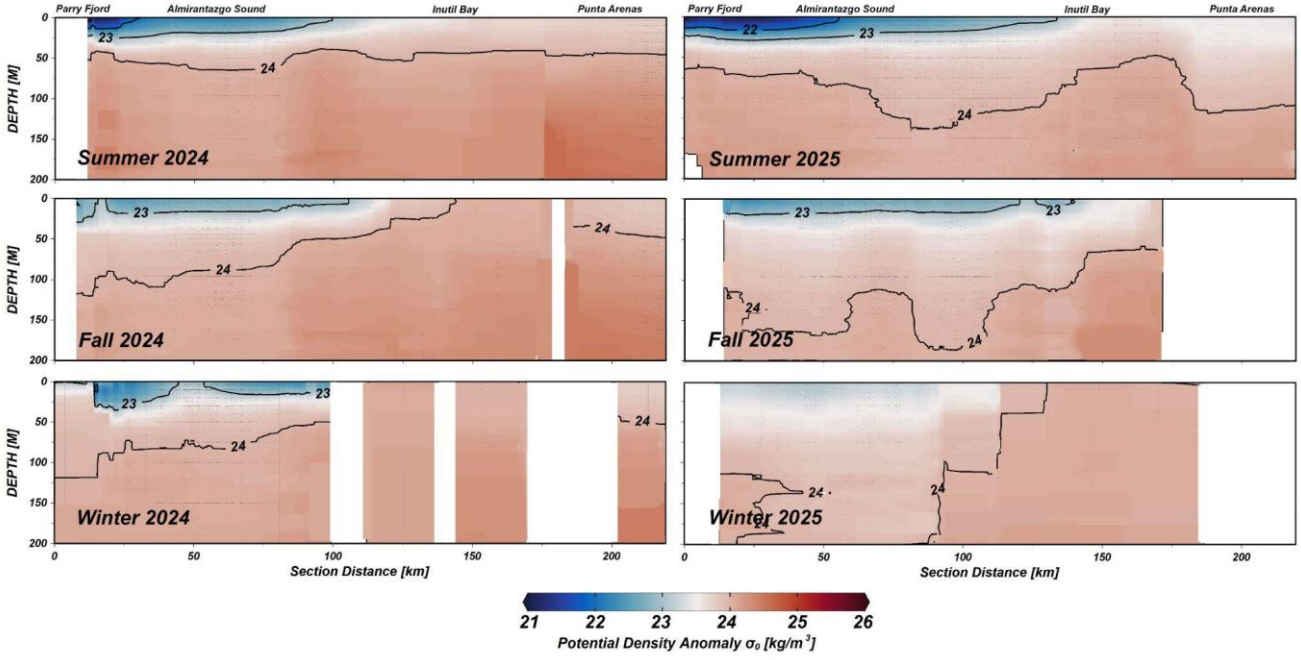

Figure 5. Potential density anomaly between Parry Fjord and Punta Arenas (southern Patagonia) during summer, fall and winter 2024/25. The along-fjord distance is referenced to Parry Fjord (Fig. 1).

The Northern Patagonia, n_s index pattern suggests a spatially and seasonally highly variable regime (Fig. 6a). In the Chiloé Inner Sea, the water column remained fully mixed ($n_s < 0.1$), suggesting persistent vertical homogeneity in this area. In the other hand, Puyuhuapi Fjord exhibited a partially mixed water column ($0.1 < n_s < 1$) round year, except during summer 2023 and spring 2024, when $n_s > 1$ which indicate stratified conditions. Notably, highly stratified conditions ($n_s > 1$) were observed in specific sectors such as Comau Fjord and the Reloncaví System during spring and summer, consistent with high N^2 frequencies (Fig. 4).

https://doi.org/10.5194/egusphere-2025-5846
Preprint. Discussion started: 5 December 2025

Southern Patagonia shows n_s consistently low (< 0.2) in all stations and seasons (Fig. 6b). Along the selected transect in the inner sea of Tierra del Fuego, the water column showed fully mixed conditions in all measurements (n_s < 0.1), reflecting a persistently homogeneous vertical structure. No events of strong stratification were detected, underscoring the dominance of vertical mixing and reduced salinity-driven layering in this region.

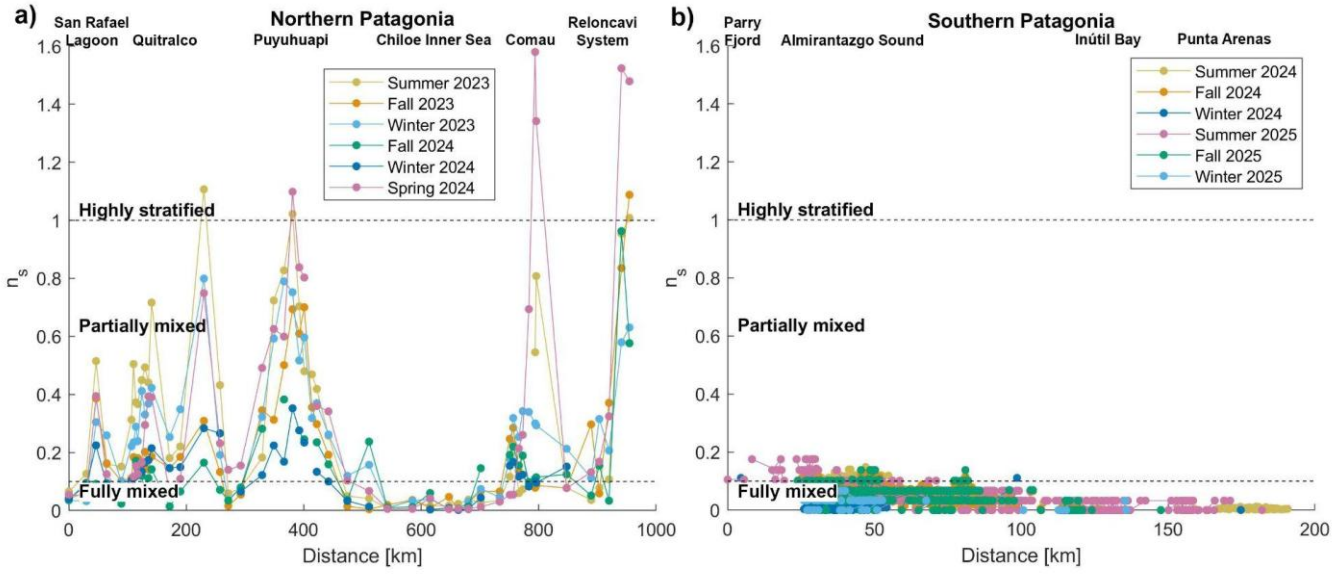

Figure 6. Stability parameters based on relative salinity differences for surveys conducted between 2023 and 2024. a) Northern Patagonia during 2023 and 2024, and b) Southern Patagonia during 2024 and 2025.

3.2 Turbulent kinetic energy dissipation rate and the vertical diffusivity coefficient

During the 2023–2024 period, studies conducted in the northern Patagonian region revealed significant variations in the turbulent kinetic energy dissipation rate (ε) and the vertical diffusivity coefficient key parameters for understanding mixing processes in fjords and channels. The data consistently showed elevated ε values in the inner sea of Chiloé, particularly in the Desertores Passage (Fig. 7), showing a persistent pattern of intensified turbulence in this area. Similarly, high dissipation rates were seen in regions characterized by topographic constrictions, such as sills and narrow passages, including Queullín Passage and the mouths of fjords like Quitralco. Vertical diffusivity coefficients were also elevated in these areas, reinforcing the presence of localized turbulent mixing.

https://doi.org/10.5194/egusphere-2025-5846
Preprint. Discussion started: 5 December 2025

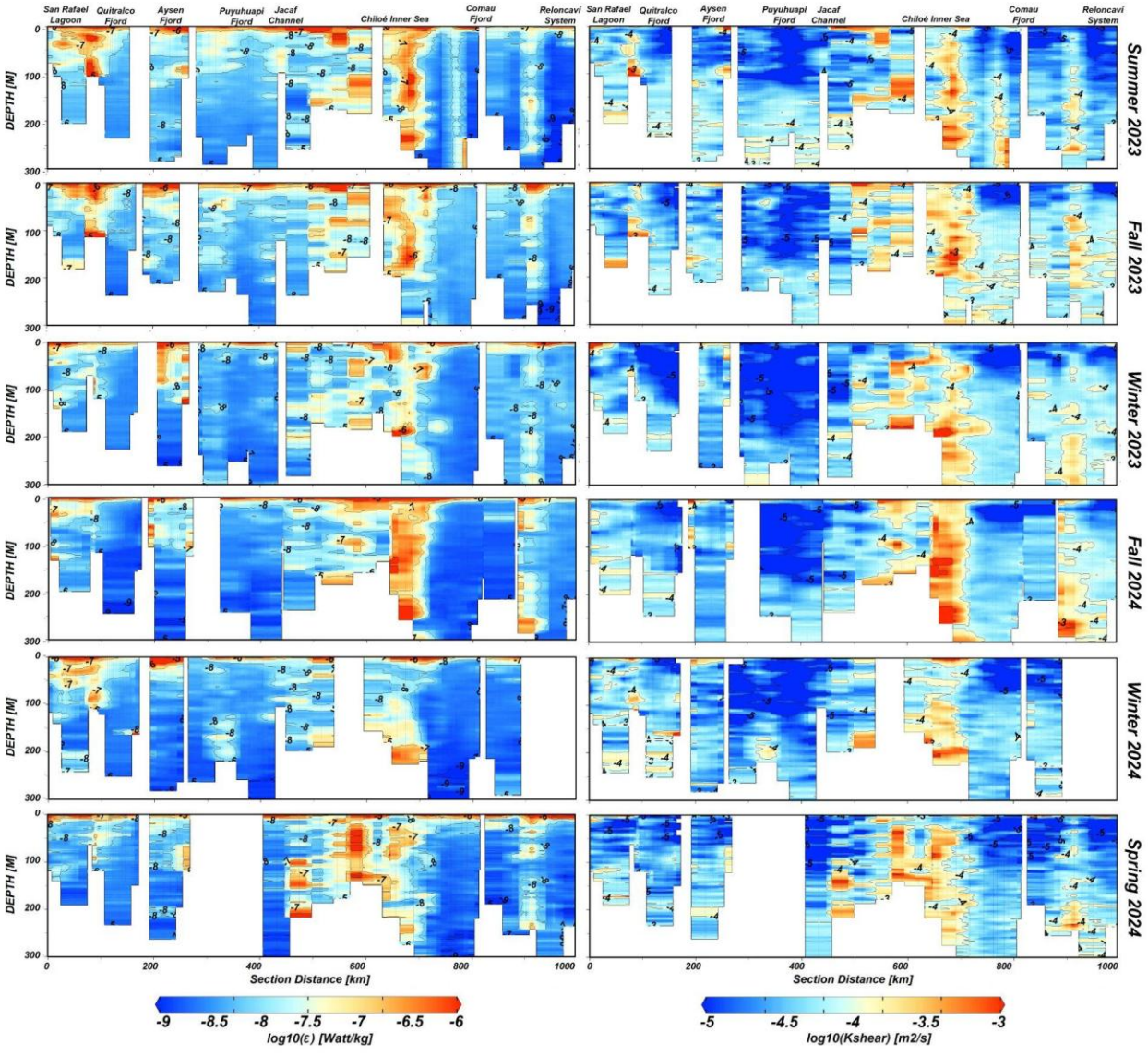

Figure 7. Comparative vertical sections of the base-10 logarithm of the mean turbulent dissipation rate (left panel) and the vertical turbulent mixing coefficient (right panel) in the Northern Patagonia region.

Turbulent kinetic energy dissipation rates (ε) reach their maximum throughout the water column at the Second Narrows, while in the other stations (Fig. 8), high values are confined to the upper 20 meters. The vertical diffusivity coefficient (K_{shear}) remains elevated along the entire transect. In Fiordo Parry and Seno Almirantazgo, ε does not show high values at depth, yet the water column exhibits a high K_{shear}. From Bahía Inútil to the First Narrows, at the Atlantic entrance, ε progressively increases along the transect.

https://doi.org/10.5194/egusphere-2025-5846
Preprint. Discussion started: 5 December 2025

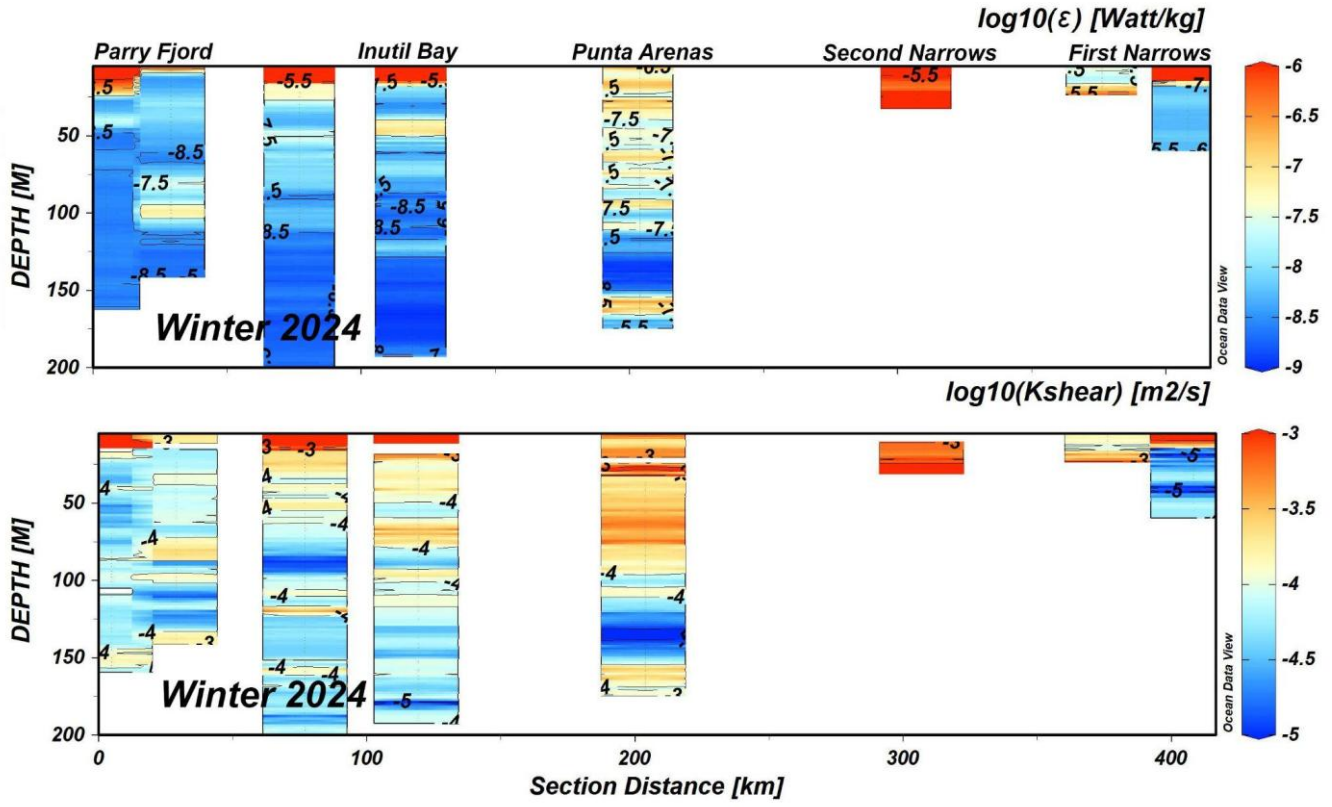

Figure 8. Vertical sections of the base-10 logarithm of the mean turbulent dissipation rate (top panel) and the vertical turbulent mixing coefficient (bottom panel) in the Southern Patagonia region during winter 2024.

3.3 Tidal mixing and energy dissipation

In Northern Patagonia, and specifically at Guafo Mouth and in the Corcovado and Ancud gulfs, high levels of tidal mixing and energy dissipation were identified. Elevated values also extend into several inner channels. In contrast, the inner reaches of confined fjords and deeper basins appear in blue tones, corresponding to areas of low dissipation (log_{10}[W m^{-2}] ≈ –8 to –11). The wind analysis derived from ERA5 reanalysis data (https://cds.climate.copernicus.eu/datasets/) averaged over 2022–2025 (without considering seasonal variability), indicate prevailing northwesterly to westerly winds with moderate intensities ranging from 4 to 8 $m\ s^{-1}$, occasionally exceeding 9 $m\ s^{-1}$ near exposed coastal areas. These winds tend to weaken toward the inner fjords (≈3–5 $m\ s^{-1}$). In this sector, semidiurnal constituents account for approximately 97% of the total dissipated energy, underscoring their dominant role in local tidal dynamics.

https://doi.org/10.5194/egusphere-2025-5846
Preprint. Discussion started: 5 December 2025

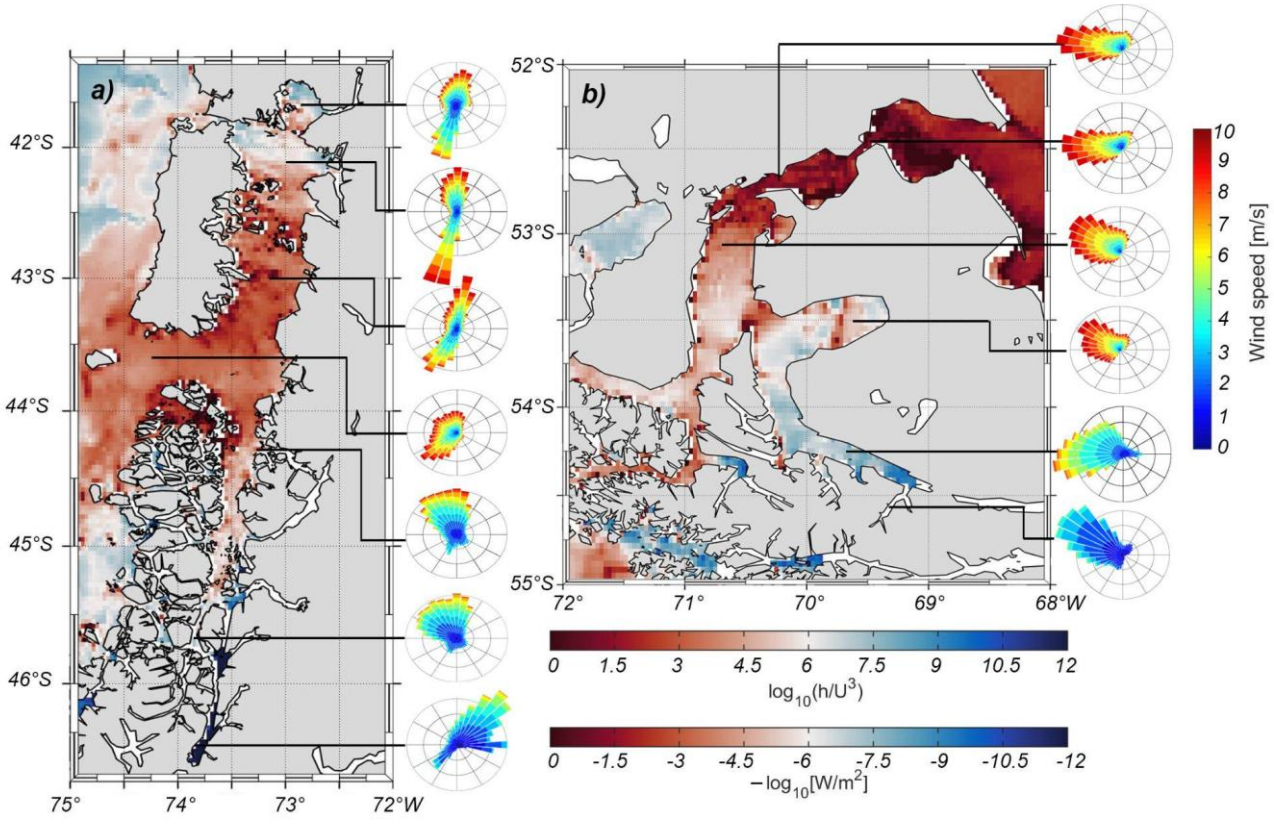

Figure 9. Spatial distribution of the tidal mixing parameter ($\log_{10}[h/U^3]$) and tidal energy dissipation ($-\log_{10}$[W m^{-2}]) in (a) Northern Patagonia and (b) Southern Patagonia. Red shading indicates regions of strong tidal mixing and dissipation, while blue represents weaker mixing. Wind roses in the side panels show the magnitude and direction (meteorological convention) of local winds for each region.

In Southern Patagonia, high mixing and dissipation values (dark reds) are observed in the eastern sector of the Strait of Magellan and toward its connection with the Atlantic. Elevated values also occur in some channels of the region. Conversely, in Almirantazgo Fjord and Parry Fjord, lower dissipation levels were observed, with values around log_{10}[W m^{-2}] ≈ –7 to –10.5, indicating limited tidal energy transfer in these deep and confined basins. Toward the southeast, in more open basins, tidal influence decreases, with wide areas of low values. In this region, wind roses (also based on ERA5 reanalysis, 2022–2025 mean fields) show stronger and more persistent winds than in the north, with magnitudes reaching 8–10 $m\,s^{-1}$ and

https://doi.org/10.5194/egusphere-2025-5846
Preprint. Discussion started: 5 December 2025

prevailing directions from the west–southwest to west–northwest. Locally, wind intensities decrease to 4–6 $m\,s^{-1}$ in more sheltered interior channels. Semidiurnal constituents account for about 76.8% of the dissipated energy, highlighting the regional contrast compared with Northern Patagonia.

4 Discussion

4.1 Sources of variability of estuarine circulation in Patagonia

Most of the studies in semi-enclosed basins like fjords and channels have been focused on the circulation patterns and their drivers (e.g., Stigebrandt, 2012). The physical mechanisms that govern the estuarine circulation have been widely studied since the early 50s (e.g., Stommel and Farmer, 1953; Pritchard, 1956). In the Patagonia fjords system, studies have shown that the main driver of the residual circulation is the pressure gradient due to freshwater input from river discharge (e.g. Davila et al., 2002; Valle-Levinson et al., 2007; Calvete and Sobarzo, 2011). The physical oceanography studies in Chilean fjords, have shown some of the forcing that modulated the estuarine circulation, wind-stress (e.g. Moffat, 2014; Soto-Riquelme et al., 2023), earth's rotation (e.g. Castillo et al., 2012), bathymetric constraint (e.g. Caceres et al., 2003), tides (e.g. Valle-Levinson et al., 2014; Ross et al., 2014), but little is known about the source of interior and deep mixing in the fjord region of Chile. A significant contribution to understanding mixing processes in Chilean fjords has been the study of the double-diffusion convective mechanism called layering. A quantification of layering showed that it occurs in deep waters of southern Patagonia. On the contrary, layering was less important in northern Patagonia and primarily restricted to the upper layers (Pérez-Santos et al., 2014; Ross et al., 2014; Pérez-Santos et al., 2018). In deep layers of Chilean fjords, the presence of constriction-sills produces the sinking of sub-surface waters into micro-basins which favor the mixing and ventilation of the deep basins (Silva and Vargas, 2014). Beyond observational work, numerical modelling has provided deeper insights: for example, Ruiz et al. (2021) used a hydrodynamic model to propose a stratified/mixed-based classification of the fjord region (seasonal stratified zones in the Moraleda Channel; permanently stratified zones in Reloncaví and Puyuhuapi fjords; and permanently mixed zones at the Guafo mouth). Moreover, internal seiche oscillations forced by wind stress have been documented in the Reloncaví Fjord, potentially contributing to vertical mixing (Castillo et al., 2017). On a biogeochemical front, Crosswell et al. (2022) showed that geophysical controls (river input, wind, tides) modulate metabolic cycling in Patagonian fjords in contrasting

https://doi.org/10.5194/egusphere-2025-5846
Preprint. Discussion started: 5 December 2025

ways depending on fjord geomorphology, highlighting that double-diffusive mixing (salt fingering) and vertical mixing are key in mediating nutrient and carbon fluxes.

4.2 Enhancing the spatial/temporal coverage of the measurements in Patagonia

This study integrates hydrographic data from oceanographic campaigns with records obtained using CTD-SRDLs deployed on elephant seals, thereby combining traditional ship-based observations with autonomous animal-borne platforms. These data increase the spatial and temporal coverage in Patagonian fjords and channels, providing an unprecedented amount of information in one of the most remote and logistically complex regions in Patagonia. The use of CTD-SRDL data significantly improves the coverage of regions poorly sampled by traditional methods (Treasure et al., 2017), and this type of in situ dataset has become one of the most abundant sources of oceanographic information at high latitudes (Smith et al., 2019), substantially contributing to reducing observational gaps in both Arctic (Blanchet et al., 2015) and Antarctic regions (Meredith et al., 2011; Piñones et al., 2019; Hückstädt et al., 2020; Roquet et al., 2013). Complementing these large-scale hydrographic observations, this study also uses microprofiler casts to evaluate the mixing processes in the Patagonian fjord region. Previous research focused on the turbulent processes that ventilate near-bottom waters (Perez-Santos et al., 2018; Linford et al., 2023) and identified the seasonality of deeper water masses which promote the advection of oxygen-rich waters into the deep basins of the fjords. By combining autonomous CTD-SRDL profiles with high-resolution microprofiler measurements, this approach strengthens the regional understanding of turbulent processes across a heterogeneous semi-enclosed coastal system (e.g., Nicholson et al., 2021).

4.3 Stratification conditions within the fjords: a comparison between northern and southern Patagonia.

The Patagonian fjords can be broadly described as an extensive estuarine system, characterized by the presence of two distinct layers: a cold, low-salinity surface layer influenced by runoff and glacial melt, and a warmer, saltier deeper layer of oceanic origin (Dyer, 2019; Bianchi, 2020; Silva & Vargas, 2014). In northern Patagonia, this estuarine structure is consistently observed throughout the study period, with the region subdivided into three main basins due to topographic constraints: (i) from Laguna San Rafael to Canal Moraleda, (ii) between Canal Moraleda and Paso Desertores, and (iii) from Paso Desertores

https://doi.org/10.5194/egusphere-2025-5846
Preprint. Discussion started: 5 December 2025

to the Reloncaví–Comau sector. The lowest densities (< 24 kg m^{-3}) occur between Laguna San Rafael and Canal Moraleda, reflecting the strong freshwater influence from glacial discharge. Between, Canal Moraleda and Paso Desertores, higher densities are recorded, associated with the intrusion of more saline oceanic waters entering through Guafo Mouth and extending into Puyuhuapi Fjord (Linford et al., 2023). Southward from Paso Desertores to the Reloncaví–Comau area, maximum densities are around 25 kg m^{-3}, while the upper 10 m remain dominated by low-density waters (< 21 kg m^{-3}) throughout the entire section. An exception is observed at Paso Desertores, where the water column remains vertically homogeneous and completely mixed across seasons (Fig. 6a).

In contrast, southern Patagonia exhibits a more variable vertical structure. During winter, the characteristic two-layer pattern typical of estuarine systems is not clearly identified, as the First and Second Narrows restrict the inflow of dense, saline oceanic waters into the Strait. As a result, the maximum salinities observed in this region do not exceed 32 g kg^{-1} (Brun et al., 2020; Valdenegro & Silva, 2003), yielding low densities (<25 kg m^{-3}) and weak vertical gradients that favor efficient vertical mixing throughout the water column (Fig. 8). During the summer, the influx of less saline surface waters favors stratification in Parry Fjord and Admiralty Fjord; however, the stratification parameter based on surface salinity and salinity at 50 m does not effectively reflect this seasonal stratification due to the limited salinity range in the area. From Punta Arenas to Bahía Inútil, the persistent vertical homogeneity is reinforced by strong tidal currents and prevailing westerly winds, which together intensify mechanical mixing and continuously erode surface buoyancy anomalies (Simeone et al., 2018; Schneider et al., 2014). The narrow geometry of the fjord acts as an energy barrier, where a large fraction of the Atlantic tidal energy is dissipated by bottom friction and internal wave breaking (Pantoja et al., 2011). Consequently, the fjords and channels south of Inútil Bay remain dominated by low salinity and low-density waters, which exhibit weak vertical gradients and limited deep renewal (Castillo et al., in review; Aravena et al., 2025).

https://doi.org/10.5194/egusphere-2025-5846
Preprint. Discussion started: 5 December 2025

4.4 Mixing in highly stratified coastal systems

4.4.1 Tidal mixing

To further interpret these spatial patterns, the distribution of tidal energy dissipation was evaluated using the tidal mixing parameter h/U^3, following the formulation of Yao et al. (2012), where h represents local depth and U the depth-averaged tidal velocity. According to Egbert and Erofeeva (2002), tides are not just a source of noise; studies of ocean microstructure have shown a correlation between turbulent dissipation rates and tidal cycles, and there is increasing evidence that tides can provide a significant source of energy for deep-ocean mixing. This framework is particularly relevant in fjord systems, where barotropic forcing interacts strongly with steep bathymetry, producing localized and persistent hotspots of turbulent dissipation.

Tidal dynamics exhibit a well-known latitudinal dependence that influences the generation, propagation, and dissipation of tidal energy. Critical latitudes, defined as those where the inertial frequency matches the tidal frequency modulate internal tide generation, the efficiency of energy transfer across harmonics, and the development of sub-harmonic instabilities (Robertson et al., 2017). Near these latitudes, internal tides may become trapped and benthic boundary layers thicken, enhancing mixing and altering the vertical structure of dissipation. Although semidiurnal internal tides (particularly M_2) display weaker latitudinal sensitivity than diurnal components, they dominate the barotropic and baroclinic tidal response in mid- and high-latitude regions. In Chilean Patagonia, this dominance aligns with the modeled spatial pattern of dissipation: the semidiurnal tide accounts for approximately 97% of the total tidal energy dissipated in northern Patagonia and 76.8% in the south, underscoring the central role of M_2 in sustaining regional turbulent mixing. This result is consistent with recent high-resolution observations in Reloncaví Sound, where semi-diurnal variability dominates current velocities, vertical shear and stratification fluctuations (Pérez-Santos et al., 2025).

The strongest tidal energy dissipation occurs in zones where bathymetric constriction amplifies current velocities, such as the Gulf of Ancud, Seno de Reloncaví, and the Magellan Strait entrances (First and Second Narrows). This spatial pattern is consistent with previous studies showing that sharp bathymetric gradients, sill-like structures, and narrow passages concentrate barotropic tidal energy and enhance vertical mixing (Castillo et al., 2016; Artal et al., 2019). Similar mechanisms have been

https://doi.org/10.5194/egusphere-2025-5846
Preprint. Discussion started: 5 December 2025

documented in other high-latitude fjord systems, including southeast Alaska (Cummins et al., 2003) and western Norway (Støylen & Fer, 2014), where strong tidal jets and internal tide conversion at constrictions generate elevated dissipation near sills and channel throats. These analogs reinforce that the hotspots identified in Patagonia arise from universal dynamical controls, namely, resonance-enhanced barotropic forcing in semi-enclosed basins and efficient energy conversion to turbulence in narrow passages providing strong external support for the modeled dissipation patterns reported here.

4.4.2 Pattern of winds-stress in Patagonia

Winds-stress is a source of mixing in the water column, the wind energy to mix the water column has been estimated with $d\varphi_W/dt$ (e.g. Denman and Miyake, 1973) which is proportional to the cubic of the wind-magnitude. The relation has been used by Jackson et al., (2025) to determine the capacity of the wind to mix the water column and enhance the deep dissolved oxygen concentration in Juan Perez Sound (British Columbia) as deep as 350 m. In the Almirantazgo Fjord, a companion study shows that the energy of the wind $d\varphi_W/dt$ was like the energy of the stratification during summer, which was evidence that the wind-stress can mix the stratified water column.

In contrast to the study of Sundfjord et al., (2017) made in Kongsfjorden in Svalbard where winter winds were at least 70% higher than in summer. The regional winds in Tierra del Fuego registered greater magnitude during summer than winter, exceeding 15 m s^{-1} within the Almirantazgo Fjord (Castillo et al., in review; Aravena et al., 2025). In southern Patagonia, the seasonality is marked in the magnitude but not in direction (westerlies round year) due to the dominance of the Southern Annular Mode (SAM) (Garreaud et al., 2013; Goyal et al., 2021). In northern Patagonia the winds change seasonality in both magnitude and direction due to the South Pacific Anticyclone (SPA); this explains the marked seasonality within the inner-sea of Chiloé (Soto-Riquelme et al., 2023). The complex-topography of Magellan region with the Darwin Cordillera and the glacial field associated, interact with SAM-driven patterns which increase the magnitude of the winds in the region (Schneider et al., 2003) in a phenomenon typical of fjord-system as orographic channeling thus amplify westerlies during SAM-positive phase (Fyfe, 2005; Goyal et al., 2021). Teleconnection between SAM and the local winds could be a positive feedback mechanism for the Magellan region, which enhances mixing on the study region.

https://doi.org/10.5194/egusphere-2025-5846
Preprint. Discussion started: 5 December 2025

4.5 Turbulent kinetic energy dissipation rate

Turbulent kinetic energy dissipation (ε) measured from microstructure profiles revealed strong spatial variability across the Patagonian fjords, largely modulated by stratification and bathymetry. Higher ε values (10^{-6}–10^{-5} $W\ kg^{-2}$,) were consistently observed near constrictions, sills, and narrow passages such as Desertores in northern Patagonia and the First and Second Narrows in the south indicating intense bottom-generated turbulence associated with tidally driven shear and topographic roughness (Figs. 7–8). In contrast, stratified basins and interior fjord areas exhibited weaker vertical diffusivities (K_{shear}. ≈ 10^{-6}–10^{-5} m² s), where the available turbulent energy is insufficient to overcome buoyancy forces and promote efficient vertical mixing (Howland et al., 2020).

Using the observed density profiles, the northern Patagonian fjords were subdivided into three sections (PN-1, PN-2, and PN-3), which reveal distinct turbulence characteristics. In PN-1 (Reloncaví–Desertores, including Comau Fjord), $\log_{10}(\varepsilon)$ is concentrated between –9.5 and –8.5, with a mode near –8.5 and relative frequencies of 40–45% during the winter 2024 campaign; extreme values occasionally reach –6 (<5%). Corresponding $\log_{10}$ (K_{shear}) values range from –5.5 to –3.5, with a mode between –4.5 and –4 and maximum frequencies of 15–25%, reflecting moderate bottom-generated mixing. PN-2 (Desertores–Moraleda Channel, including Puyuhuapi and Apiao Channel) exhibits a similar ε range (–9.5 to –7.5) but with less pronounced peaks and slightly lower maximum frequencies (20–30%), while K_{shear} modes remain comparable to PN-1, suggesting relatively homogeneous conditions with fewer extreme events. PN-3 (Moraleda Channel–Laguna San Rafael, including Quitralco) displays the highest turbulence intensities, with winter 2024 frequencies reaching ~50% at –8.5 and occasional high ε values up to –6, accompanied by K_{shear} values extending toward –3.3, indicating a more vigorous mixing regime. In the southern basins, PS-1 (Magellan Strait–Parry Fjord, Atlantic sector) shows lower occurrence of high ε values (≥–7) relative to northern basins, with K_{shear} modes near –4.3 and frequencies of 20–25%, consistent with a weaker mixing regime shaped by reduced tidal energy and stronger stratification. Overall, these distributions highlight that PN1 and PN2 represent moderately mixed fiords, PN3 acts as a transition zone with more energetic turbulence, and the southern basins (PS1–PS2) are generally more strongly mixed, with higher vertical diffusivities reflecting both tidal forcing and less persistent stratification (Fer et al., 2018; Staalstrøm & Røed, 2016).

https://doi.org/10.5194/egusphere-2025-5846
Preprint. Discussion started: 5 December 2025

Although with different density structures, the efficiency of mixing decreases under strong stratification. In such conditions, a larger fraction of the available energy is expended in maintaining internal wave motions rather than producing irreversible mixing (Stretch et al., 2010). Conversely, when stratification is weak, the same turbulent energy leads to more efficient vertical exchange, resulting in higher diffusivity and homogenization of the water column. This relationship is consistent with the observed vertical distribution of ε and K_{shear}, where enhanced values typically occur near the seabed and pycnocline interfaces, reflecting localized shear instabilities that modulate energy transfer within the water column (consistent with observations in other fjords such as Saanich Inlet and Norwegian fjords; Rippeth et al., 2002; Fer et al., 2018).

Notably, the regions exhibiting the highest dissipation measured with the microprofiler coincide with the areas of maximum tidal energy loss estimated from the Yao et al. (2012) parameterization. This spatial coherence supports the view that tidal forcing modulated by local bathymetry is the primary driver of bottom-intensified turbulence in Patagonian fjords. In these regions, strong and continuous tidal flows sustain vertically homogeneous conditions, as observed in Desertores and the First and Second Narrows, where the water column remains well mixed throughout the tidal cycle. In contrast, broader and more weakly forced basins display intermittent or seasonal mixing, often associated with wind events or internal wave breaking rather than steady tidal shear (similar patterns have been reported in Norwegian fjords and the Gulf of Alaska, highlighting the role of local topography in modulating turbulence; MacCready & Geyer, 2010; Stigebrandt, 2012).

These findings highlight that the contrasting hydrographic regimes of northern and southern Patagonia result from the combined influence of bathymetric control, tidal intensity, and freshwater forcing. By modulating the balance between stratification and vertical exchange, these processes govern deep-water renewal, oxygenation, and nutrient supply that sustain Patagonian fjord ecosystems and their sensitivity to future climatic variability.

https://doi.org/10.5194/egusphere-2025-5846
Preprint. Discussion started: 5 December 2025

5 Conclusions

This study reveals that the fjords and channels of Patagonia exhibit pronounced regional contrasts in hydrographic structure and turbulent mixing, governed by the interplay between tidal forcing, winds, bathymetry, and freshwater inputs. In northern Patagonia, a persistent two-layer estuarine system is maintained throughout the year, with stratification modulated by glacial discharge and oceanic intrusions. Within this region, sills and constricted passages such as Desertores act as energetic mixing hotspots, where strong tidal currents interacting with rough topography generate intense bottom turbulence and promote vertical homogenization. In contrast, the southern Patagonia displays a weaker and more variable stratification, where the restricted inflow of dense oceanic waters and the dominance of strong tidal currents and westerly winds sustain vertically homogeneous conditions, particularly across the First and Second Narrows.

Microstructure measurements demonstrate that spatial patterns of turbulent kinetic energy dissipation (ε) closely follow the distribution of tidal energy loss predicted by the tidal mixing parameter h/U^3, confirming that semidiurnal tides especially the M_2 constituent are the main driver of turbulence across the region. Under weak stratification, tidal shear leads to efficient vertical exchange, while in strongly stratified basins, a greater fraction of energy is trapped in internal motions rather than producing irreversible mixing. Consequently, bathymetric constrictions not only enhance turbulence generation but also regulate the vertical transfer of energy, determining whether the water column remains stratified or well mixed.

https://doi.org/10.5194/egusphere-2025-5846
Preprint. Discussion started: 5 December 2025

APENDIX A

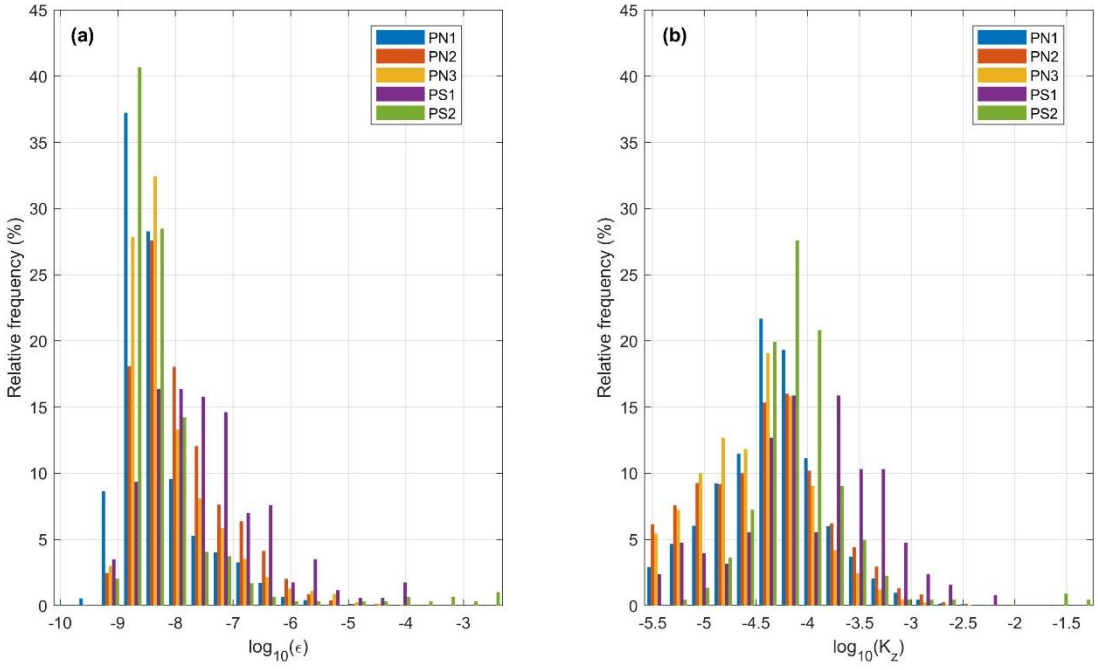

Figure A1. Inter-basin comparison of the relative frequency distributions of turbulent kinetic energy dissipation ($\log_{10}\varepsilon$; panel a) and shear-derived vertical diffusivity ($\log_{10}K_{shear}$; panel b). Colors represent the five basin groups: PN1 (Reloncaví–Desertores, including Comau Fjord), PN2 (Desertores–Moraleda, including Puyuhuapi fjords), PN3 (Moraleda–Laguna San Rafael, including Quitralco Fjord), PS1 (Atlantic entrance of the Strait of Magellan to Punta Arenas), and PS2 (Bahía Inútil to Parry Fjord).

https://doi.org/10.5194/egusphere-2025-5846
Preprint. Discussion started: 5 December 2025

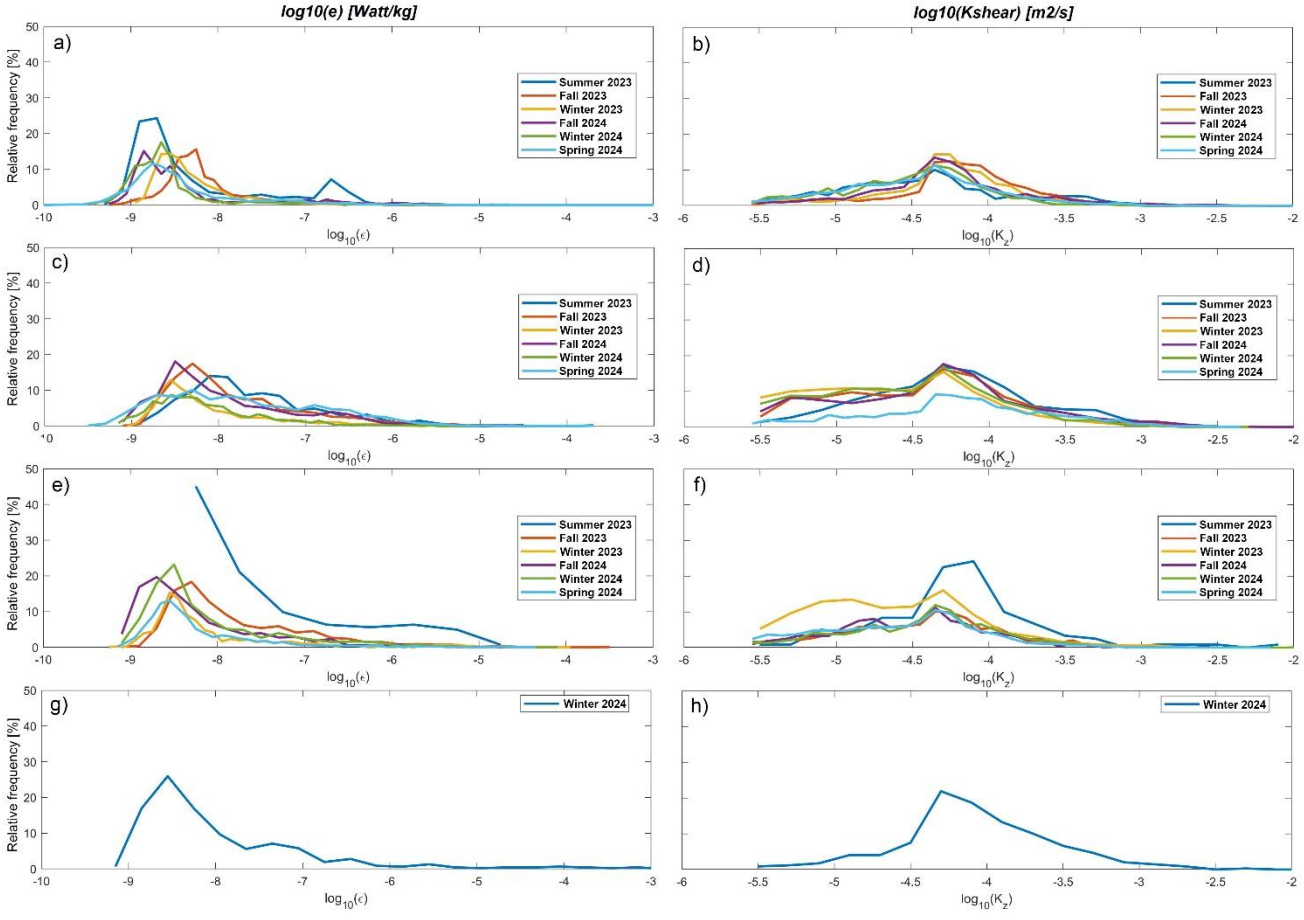

Figure A2. Relative frequency distributions of turbulent kinetic energy dissipation ($\log_{10}\varepsilon$) and shear-derived vertical diffusivity ($\log_{10}K_{shear}$) for all oceanographic campaigns between 2023 and 2024. Panels (a, c, e, g) show the variability in ε, while panels (b, d, f, h) display the corresponding K_{shear} distributions

https://doi.org/10.5194/egusphere-2025-5846
Preprint. Discussion started: 5 December 2025

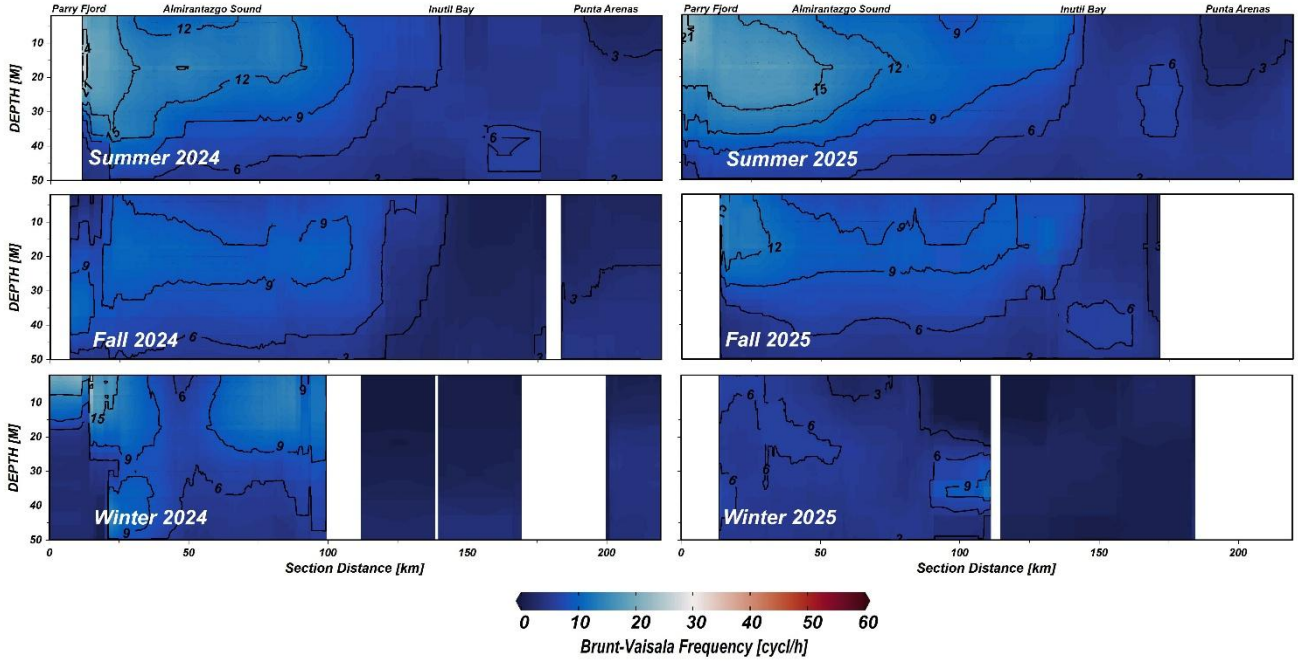

Figure A3. Brunt-Väisälä frequency (first 50 m) along the southern Patagonia region for summer, fall and winter and of 2024/25. The along-fjord distance is referenced to San Rafael lagoon (Fig. 1).

Authors contribution

MRC, IPS, MIC, designed the study and wrote the initial manuscript draft. MS, MFL, AP, CBG, AG and JG-V contribute to improving the subsequent versions of the manuscript. MRC, IPS, MIC wrote codes and made data analysis. Discussions and iterative feedback from all co-authors significantly contributed to the revision of the manuscript.

Competing interests

The authors declare that they have no conflict of interest.

Acknowledgements

This study was supported by ANID/ANILLO/ATE220033 project. Ship-based and turbulence data was carried out by CIMAR 27F 24-06 and IFOP-Chile cruises. IPS was funded by FONDECYT 1251038 and COPAS COASTAL FB210021. JGV acknowledges FONDAP N° 15150003. MIC thanks to FONDEF ID22I10206. MS acknowledges FONDECYT 1231058. This work forms part of the academic portfolio of MIC for full professorship at the University of Valparaíso (UV).

https://doi.org/10.5194/egusphere-2025-5846
Preprint. Discussion started: 5 December 2025

Code and Data Availability Statement

The datasets used open source and are available online: hourly ERA 5 wind data is available at https://cds.climate.copernicus.eu/datasets/reanalysis-era5-single-levels?tab=download, sealevel data at https://www.ioc-sealevelmonitoring.org/, tidal model is available by request at https://github.com/chadagreene/Tide-Model-Driver. The wind data from meteorological stations along Chile is available at https://climatologia.meteochile.gob.cl/application/requerimiento/producto/RE3008. All data will be upload to the National Oceanographic Center of Chile (https://cendhoc.shoa.cl/inicio). All scripts used to obtain the results presented in this study could be shared upon request at the corresponding author.

References

Aiken, C. M.: Temporal variability of the semidiurnal tide in the Chilean Inland Sea, Cont. Shelf Res., 28(2), 168–182, doi:10.1016/j.csr.2007.08.008, 2008.

Aravena-Yáñez, V., Garcés-Vargas, J., and Benavides-Martínez, I. F.: Freshwater plume's impact on the thermohaline structure of the water column in the Central Zone of the Strait of Magellan, Regional Studies in Marine Science, 83, 104087, doi:10.1016/j.rsma.2025.104087, 2025.

Arneborg, L., Liljebladh, B., Stigebrandt, A., Fiekas, V., and Umlauf, L.: The rate of inflow and mixing during deep water renewal in a silled fjord, Limnol. Oceanogr., 49(3), 768–777, doi:10.4319/lo.2004.49.3.0768, 2004.

Baker, E. T., Walker, S. L., Massoth, G. J., and Berkenbosch, H. A.: Water column structure and biogeochemical signatures in Patagonian fjords, Prog. Oceanogr., 193, 102534, doi:10.1016/j.pocean.2021.102534, 2021.

Bendtsen, J., Rysgaard, S., Carlson, D. F., Meire, L., and Sejr, M. K.: Vertical mixing in stratified fjords near tidewater outlet glaciers along northwest Greenland, J. Geophys. Res. Oceans, 126(8), doi:10.1029/2020jc016898, 2021.

Bianchi, T. S., Arndt, S., Austin, W. E. N., Benn, D. I., Bertrand, S., Cui, X., Faust, J. C., Koziorowska-Makuch, K., Moy, C. M., Savage, C., Smeaton, C., Smith, R. W., and Syvitski, J.: Fjords as aquatic critical zones (ACZs), Earth-Sci. Rev., 203, 103145, doi:10.1016/j.earscirev.2020.103145, 2020.

Blanchet, M. A., et al.: Elephant seals provide oceanographic observations. Marine Ecology Progress Series, 519, 213–230, https://doi.org/10.3354/meps11088, 2015.

https://doi.org/10.5194/egusphere-2025-5846
Preprint. Discussion started: 5 December 2025

Boehme, L., Lovell, P., Biuw, M., Roquet, F., Nicholson, J., Thorpe, S. E., Meredith, M. P., and Fedak, M. A.: Technical note: Animal-borne CTD-Satellite Relay Data Loggers for real-time oceanographic data collection, Ocean Sci., 5, 685–695, doi:10.5194/os-5-685-2009, 2009.

Brun, A. A., Ramirez, N., Pizarro, O., and Piola, A. R.: The role of the Magellan Strait on the southwest South Atlantic shelf. Estuarine, Coastal and Shelf Science, 237, https://doi.org/10.1016/j.ecss.2020.106661, 2020

Cáceres, M., Valle-Levinson, A., and Castillo, M.: Tidal asymmetry and turbulence in a Chilean fjord, Estuar. Coast. Shelf Sci., 56(5–6), 767–778, doi:10.1016/S0272-7714(02)00301-5, 2003.

Carranza, M. M., Gille, S. T., Piola, A. R., Charo, M., and Romero, S. I.: Wind modulation of upwelling at the shelf-break front off Patagonia: Observational evidence. Journal of Geophysical Research: Oceans, 122(3), 2401–2421, https://doi.org/10.1002/2016JC012059, 2017.

Carter, G. S., Gregg, M. C., and Kunze, E.: Internal waves, solitary-like waves, and mixing on the Monterey Bay shelf, Cont. Shelf Res., 28(7), 771–779, doi:10.1016/j.csr.2007.12.012, 2008.

Castillo, M., Schneider, W., and Sievers, H.: Mixing processes in the Chiloé Inland Sea, Chile, Cont. Shelf Res., 42, 1–12, doi:10.1016/j.csr.2012.05.005, 2012.

Crosswell, J. R., et al.: Controls on carbon and nutrient cycling in Patagonian fjords. Marine Chemistry, 235, 104064, https://doi.org/10.1016/j.marchem.2021.104064
, 2022.

Dávila, P. M., Figueroa, D., and Müller, E.: Freshwater input into the coastal ocean and its relation with the salinity distribution off austral Chile (35–55°S), Cont. Shelf Res., 22(3), 521–534, doi:10.1016/S0272-7714(01)00072-3, 2002.

Devine, M.: Some features of the dynamic structure of a deep estuary, Estuar. Coast. Shelf Sci., 16, 271–289, doi:10.1016/0272-7714(83)90145-2, 1983.

Dyer, K.: Estuarine Circulation, Encyclopedia of Ocean Sciences, Third Edition: Volume 1-5, 1–5, V6-67-V6-73, https://doi.org/10.1016/B978-0-12-409548-9.11427-7, 2019.

https://doi.org/10.5194/egusphere-2025-5846
Preprint. Discussion started: 5 December 2025

Egbert, G. D., and Erofeeva, S. Y.: Efficient inverse modeling of barotropic ocean tides, Journal of Atmospheric and Oceanic Technology, 19, 183–204, doi:10.1175/1520-0426(2002)019<0183:EIMOBO>2.0.CO;2, 2002.

Farmer, D. M. and Freeland, H. J.: The physical oceanography of fjords, Prog. Oceanogr., 12, 147–219, 1983.

Fedak, M., Lovell, P., McConnell, B., and Hunter, C.: Overcoming the constraints of long-range radio telemetry from animals: Getting more useful data from smaller packages, Integr. Comp. Biol., 42(1), 3–10, doi:10.1093/icb/42.1.3, 2002.

Ferron, B., Bouruet-Aubertot, P., Cuypers, Y., and Finite, M.: Turbulent mixing in fjords: Variability and drivers. Progress in Oceanography, 128, 30–48, 2014.

Field, I. C., Harcourt, R. G., Boehme, L., de Bruyn, P. J. N., Charrassin, J. B., McMahon, C. R., Bester, M. N., Fedak, M. A., and Hindell, M. A.: Refining instrument attachment on phocid seals, Marine Mammal Science, 28, E325–E332, doi:10.1111/j.1748-7692.2011.00519.x, 2012.

Gregg, M. C. Diapycnal mixing in the thermocline: A review. Journal of Geophysical Research, 92(C5), 5249–5286, 1987.

Haralambidou, K., Georgiou, D., and Krestenitis, Y.: Assessment of water column stratification in coastal environments using in situ data. Journal of Marine Systems, 82, 254–270, 2010.

Howland, C. J., Taylor, J. R., and Caulfield, C. P.: Mixing in forced stratified turbulence and its dependence on large-scale forcing, Journal of Fluid Mechanics, 890, A18, doi:10.1017/jfm.2020.152, 2020.

Hückstädt, L. A., et al.: Marine mammals as ocean sensors. Annual Review of Marine Science, 12, 61–87, https://doi.org/10.1146/annurev-marine-010419-011132, 2020.

Inall, M. E. and Gillibrand, P. A.: The physics of mid-latitude fjords: A review, Geological Society, London, Special Publications, 344(1), 17–33, 2010.

IOC, SCOR, and IAPSO: The international thermodynamic equation of seawater – 2010: Calculation and use of thermodynamic properties, Intergovernmental Oceanographic Commission, Manuals and Guides, No. 56, UNESCO (English), 196 pp., 2010.

https://doi.org/10.5194/egusphere-2025-5846
Preprint. Discussion started: 5 December 2025

Klymak, J. M. and Gregg, M. C.: The role of upstream waves and a downstream density pool in the breaking of a tall sill, J. Phys. Oceanogr., 33(4), 754–769, doi:10.1175/1520-0485(2003)033<0754:TROUWA>2.0.CO;2, 2003.

Landaeta, M. F., Suárez-Donoso, N., Bustos, C. A., Balbontín, F.: Feeding habits of larval Maurolicus parvipinnis (Sternoptychidae) in Patagonian fjords. J. Plankton Res., 33(12), 1813–1824, doi:10.1093/plankt/fbr081, 2011.

Linford, P., Narváez, D., Pérez-Santos, I., Saldías, G., Montero, P., and Altamirano, R.: Recent deoxygenation of Patagonian fjord subsurface waters connected to the Peru–Chile Undercurrent and Equatorial Subsurface Water variability, Global Biogeochemical Cycles, 37, e2022GB007688, doi:10.1029/2022GB007688, 2023.

MacKinnon, J. A., Zhao, Z., Whalen, C. B., Waterhouse, A. F., Trossman, D. S., Sun, O. M., St. Laurent, L. C., Simmons, H. L., Polzin, K., Pinkel, R., Pickering, A., Norton, N. J., Nash, J. D., Musgrave, R., Merchant, L. M., Melet, A. V., Mater, B., Legg, S., Large, W. G., Kunze, E., Klymak, J. M., Jochum, M., Jayne, S. R., Hallberg, R. W., Griffies, S. M., Diggs, S., Danabasoglu, G., Chassignet, E. P., Buijsman, M. C., Bryan, F. O., Briegleb, B. P., Barna, A., Arbic, B. K., Ansong, J. K., and Alford, M. H.: Climate Process Team on Internal Wave–Driven Ocean Mixing, Bulletin of the American Meteorological Society, 98, 2429–2454, doi:10.1175/BAMS-D-16-0030.1, 2017.

Meredith, M. P., et al.: Southern Ocean overturning circulation from seal-borne CTD data. Geophysical Research Letters, 38, L17607, https://doi.org/10.1029/2011GL048408, 2011.

Munk, W., & Wunsch, C. Abyssal recipes II: Energetics of tidal and wind mixing. Deep-Sea Research Part I, 45(12), 1977–2010, 1998.

Nash, J. D., Shroyer, E. L., Kelly, S. M., Inall, M. E., Duda, T. F., Levine, M. D., Jones, N. L., and Musgrave, R. C.: Are any coastal internal tides predictable?, Oceanography, 25(2), 80–95, doi:10.5670/oceanog.2012.44, 2012.

Nicholson, D. P., et al.: Turbulence and mixing across coastal fjords. Journal of Geophysical Research: Oceans, 126, e2020JC016, https://doi.org/10.1029/2020JC016, 2021.

Palma, S., and Silva, N.: Distribution of water masses and nutrient salts in the Strait of Magellan. Ciencia y Tecnología del Mar, 27, 47–65, 2004.

Palmer, M. R., Inall, M. E., and Sharples, J.: The physical oceanography of Jones Sound, a High Arctic fjord, Prog. Oceanogr., 122, 123–140, doi:10.1016/j.pocean.2013.11.001, 2014.

https://doi.org/10.5194/egusphere-2025-5846
Preprint. Discussion started: 5 December 2025

Panella, S., Silva, N., and Sievers, H.: Water masses and circulation in southern Chilean fjords, Bol. Soc. Biol. Concepción, 62, 49–62, 1991.

Pantoja, S., Iriarte, J. L., and Daneri, G.: Oceanography of the Chilean Patagonia, Cont. Shelf Res., 31(3–4), 149–153, doi:10.1016/j.csr.2010.10.013, 2011.

Pérez-Santos, I., Castro, L., Ross, L., Niklitschek, E., Mayorga, N., Cubillos, L., Gutierrez, M., Escalona, E., Alegría, N., and Daneri, G.: Turbulence and hypoxia contribute to dense biological scattering layers in Patagonian Fjord System, Ocean Sci. Discuss., 2018, 1–25, doi:10.5194/os-2017-89, 2018.

Pérez-Santos, I., Díaz, P. A., Ross, L., Riquelme-Bugueño, R., Lara, C., Barrera, F., Díaz-Astudillo, M., Muñoz, R., Landaeta, M., Linford, P., Rodríguez-Villegas, C., Schwerter, C., Arenas-Uribe, S., Navarro, P., Mancilla-Gutiérrez, G., Jorquera, E., Artal, O., and Saldías, G. S.: On the diurnal-semidiurnal cycles of physical and biological inter-processes in the upper water column of Reloncaví Sound, northern Patagonia, Marine Environmental Research, 212, 107482, doi:10.1016/j.marenvres.2025.107482, 2025.

Pickard, G. L.: Some physical oceanographic features of inlets of Chile, J. Fish. Res. Board Can., 28(8), 1077–1106, doi:10.1139/f71-161, 1971.

Pinilla, E., Castillo, M., Pérez-Santos, I., Venegas, O., and Valle-Levinson, A.: Water age variability in a Patagonian fjord, J. Mar. Syst., 210, 103376, doi:10.1016/j.jmarsys.2020.103376, 2020.

Piñones, A., et al.: Oceanographic connectivity in fjord ecosystems. Progress in Oceanography, 177, 101871, https://doi.org/10.1016/j.pocean.2019.05.007, 2019.

Pope, S. B. Turbulent Flows. Cambridge University Press, 2000.

Pritchard, D. W.: The dynamic structure of a coastal plain estuary. Journal of Marine Research, 15, 33–42, 1956.

Roquet, F., et al.: Estimates of the Southern Ocean general circulation from seal CTD data. Science, 330(6012), 1483–1487, https://doi.org/10.1126/science.1191220, 2013.

https://doi.org/10.5194/egusphere-2025-5846
Preprint. Discussion started: 5 December 2025

Ruiz, C., Artal, O., Pinilla, E., and Sepúlveda, H. H.: Stratification and mixing in the Chilean Inland Sea using an operational model, Ocean Modelling, 158, 101750, doi:10.1016/j.ocemod.2020.101750, 2021.

Sassi, M.G., Palma, E.D.,: Modelo Hidrodinámico del Estrecho de Magallanes. Asociación Argentina de Mecánica Computacional. Mec. Comput. XXV (16), 1461–1477, 11. https://cimec.org.ar/ojs/index.php/mc/article/view/577/550, 2006.

Schneider, W., Pérez-Santos, I., Ross, L., Bravo, L., Seguel, R., and Hernández, F.: On the hydrography of Puyuhuapi channel, Chilean Patagonia, Prog. Oceanogr., 129, 8–18, doi:10.1016/j.pocean.2014.03.007, 2014.

Scully, M. E., Friedrichs, C. T., and Brubaker, J. M.: Control of estuarine stratification and mixing by wind forcing, Estuar. Coast. Shelf Sci., 63(3), 607–618, doi:10.1016/j.ecss.2005.01.004, 2005.

Sievers, H. and Silva, N.: Water masses and circulation in the fjords of northern Patagonia, Chile, Sci. Mar., 72(3), 449–460, doi:10.3989/scimar.2008.72n3449, 2008.

Sievers, H., Silva, N., and Prado, R.: Circulación profunda y renovación de aguas en los fiordos de la Patagonia. Ciencia y Tecnología del Mar, 25, 47–58, 2002.

Silva, N. and Palma, S.: Avances en el conocimiento oceanográfico de las aguas interiores chilenas, Puerto Montt a cabo de Hornos, Comité Oceanográfico Nacional, 2008.

Silva, N. and Vargas, C. A.: Hypoxia in Chilean Patagonian fjords, Prog. Oceanogr., 129, 62–74, doi:10.1016/j.pocean.2014.05.016, 2014.

Simeone, S., Valle-Levinson, A., and Alleyne, D.: Tidal energy dissipation in the Strait of Magellan, J. Geophys. Res. Oceans, 123, 6249–6264, doi:10.1029/2018JC014196, 2018.

Simpson, J. H., and Hunter, J. R.: Fronts in the Irish Sea. Nature, 250, 404–406, https://doi.org/10.1038/250404a0, 1974.

Smith, M. S., et al.: The role of elephant seals in ocean observing systems. Frontiers in Marine Science, 6, 421, https://doi.org/10.3389/fmars.2019.00421, 2019.

Staalstrøm, A., and Røed, L. P.: Vertical mixing and internal wave energy fluxes in a sill fjord, Journal of Marine Systems, 159, 15–32, doi:10.1016/j.jmarsys.2016.02.007, 2016.

https://doi.org/10.5194/egusphere-2025-5846
Preprint. Discussion started: 5 December 2025

Stigebrandt, A.: Hydrodynamics and circulation of fjords. In: Bengtsson, L., Herschy, R. W., and Fairbridge, R. W. (Eds.), Encyclopedia of Lakes and Reservoirs, 327–344, Springer, https://doi.org/10.1007/978-1-4020-4410-6_181, 2012.

Stigebrandt, A.: Renewal of deep water in fjords by tidal exchange, J. Geophys. Res. Oceans, 123(3), 2463–2477, doi:10.1002/2017JC013263, 2018.

Stommel, H., and Farmer, H. G.: Control of salinity in an estuary by a transition. Journal of Marine Research, 12, 13–20, 1953.

Stretch, D. D., Rottman, J. W., Venayagamoorthy, S. K., Nomura, K. K., and Rehmann, C. R.: Mixing efficiency in decaying stably stratified turbulence, Dynamics of Atmospheres and Oceans, 49, 25–36, doi:10.1016/j.dynatmoce.2008.11.002, 2010.

Tennekes, H., & Lumley, J. L. (1972). A First Course in Turbulence. MIT Press.

Thorpe, S. A. The Turbulent Ocean. Cambridge University Press, 2005.

Treasure, A. M., et al.: Marine mammals exploring the oceans pole to pole. Nature Ecology & Evolution, 1, 011, https://doi.org/10.1038/s41559-016-0011, 2017.

Valdenegro, A., and Silva, N.: Caracterización oceanográfica física y química de la zona de canales australes entre Puerto Montt y Laguna San Rafael. Ciencia y Tecnología del Mar, 26, 19–60, 2003.

Valle-Levinson, A., Blanco, J. L., and Frangópulos, M.: Hydrography and mixing at a Patagonian fjord mouth, Cont. Shelf Res., 21(18–19), 2543–2555, doi:10.1016/S0272-7714(01)00108-4, 2001.

Valle-Levinson, A., Sarkar, N., Sanay, R., Soto, D., and León, J.: Spatial structure of hydrography and flow in a Chilean fjord, Estuar. Coast. Shelf Sci., 73(3–4), 654–670, doi:10.1016/j.ecss.2007.02.006, 2007.

Vargas, C. A., Martínez, R. A., Cuevas, L. A., Pavez, M. A., Cartes, C., and González, H. E.: Seasonal patterns in plankton dynamics, microplankton biomass, and hydrography in a Chilean Patagonia fjord, Estuar. Coast. Shelf Sci., 93(3), 178–189, doi:10.1016/j.ecss.2011.04.003, 2011.

Waterhouse, A. F., et al. (2014). Global patterns of diapycnal mixing from measurements of the turbulent dissipation rate. Journal of Physical Oceanography, 44(7), 1854–1872.

https://doi.org/10.5194/egusphere-2025-5846
Preprint. Discussion started: 5 December 2025

Whitney, M. M., Allen, S. E., Jones, N. L., Lerczak, J. A., and Green, J. A.: Internal waves and mixing in fjord systems, J. Geophys. Res. Oceans, 119, 5666–5689, doi:10.1002/2013JC009330, 2014.

Yao, Z., He, R., Bao, X., Wu, D., and Song, J.: M2 tidal dynamics in the Bohai and Yellow Seas: a hybrid data assimilative modeling study, Ocean Dynamics, 62, 753–769, doi:10.1007/s10236-012-0529-6, 2012.

Zaldívar, J.-M., Cardoso, A., Viaroli, P., Newton, A., De Wit, R., Ibáñez, C., Reizopoulou, S., Somma, F., Razinkovas-Baziukas, A., Basset, A., Holmer, M., and Murray, N.: Eutrophication in transitional waters: an overview, Transitional Waters Monographs, 1, 1–78, doi:10.1285/i18252273v2n1p1, 2008.